Supplementary Information

Spectroscopic Signature of Chemical Bond Dissociation Revealed by Calculated Core-Electron Spectra

Ludger Inhester,[*,†,‖] Zheng Li,[*,‡,‖] Xiaolei Zhu,[*,¶] Nikita Medvedev,[*,§] and Thomas J. A. Wolf[*,¶]

†Center for Free-Electron Laser Science, DESY, Notkestrasse 85, 22607 Hamburg, Germany

‡Max Planck Institute for the Structure and Dynamics of Matter, D-22761 Hamburg, Germany

¶Stanford PULSE Institute, SLAC National Accelerator Laboratory, 2575 Sand Hill Road, Menlo Park, CA 94025, USA

§Institute of Physics and Institute of Plasma Physics, Academy of Science of Czech Republic, Na Slovance 1999/2, 18221 Prague 8, Czech Republic

‖L.I. and Z.L. contributed equally to this work.

E-mail: ludger.inhester@cfel.de; zheng.li@desy.de; zhuxl@stanford.edu; medvedev@ipp.cas.cz; tw2809@slac.stanford.edu

In this Supplementary Information, we present details of quantum dynamical model and a comparison of calculated data for CH_3I and methane with available experimental data. We discuss the effect of finite time resolution on the observed signal. Further, we discuss the classical model of charge transfer between the core ionized carbon atom and the iodine atom,[1,2] which is adapted to our case of CH_3 and I with partial charges.

Comparison of the calculated and experimental XPS binding energies

Due to the lack of time-resolved experimental data for the photodissociation of CH_3I, we can only benchmark the quality of our results by comparison of the C 1s binding energy in the electronic ground state with experimental measurements. The experimental value of the binding energy is 291.43 eV,[3] which is in good agreement to our calculated value of 291.97 eV.

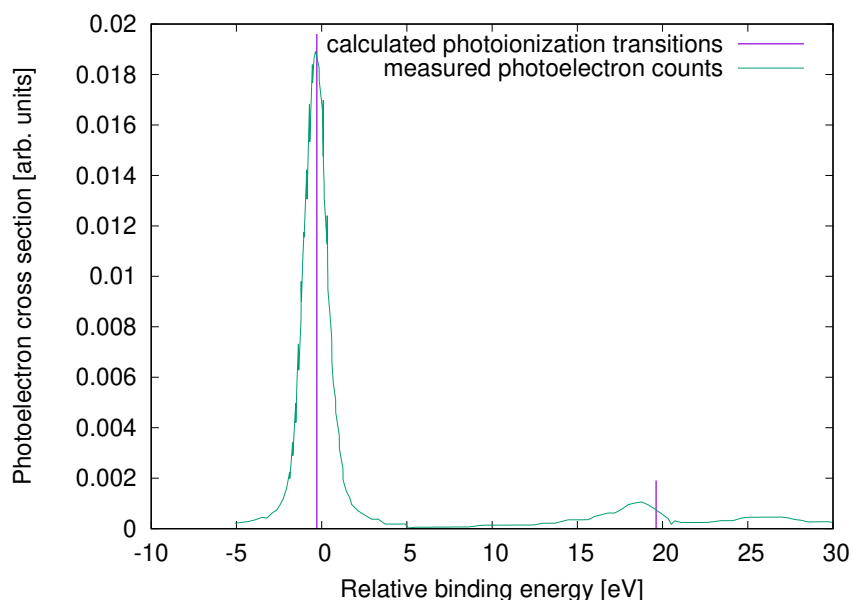# Comparison of the calculated and experimental XPS and AES spectra of methane

Figure S1: Comparison of calculated and measured XPS. Experimental data extracted from Ref. 4.

To verify our calculation procedure, we compare the XPS of methane with calculations employing the same parameters (6-311G basis set, small active space comprising the lowest bound and the nearest unbound orbitals) in Fig. S1. The measured data is extracted from Ref. 4. According to this reference, the main photoelectron line is at 290.7 eV, which is in good agreement with our

calculated value of 291.2 eV. As can be seen in Fig. S1, the calculated data indicates a shake-up satellite at 19.9 eV below the main line in good agreement with the experimental position of 18.9 eV. The relative strength of shake-up to main line are also well reproduced in the calculation.
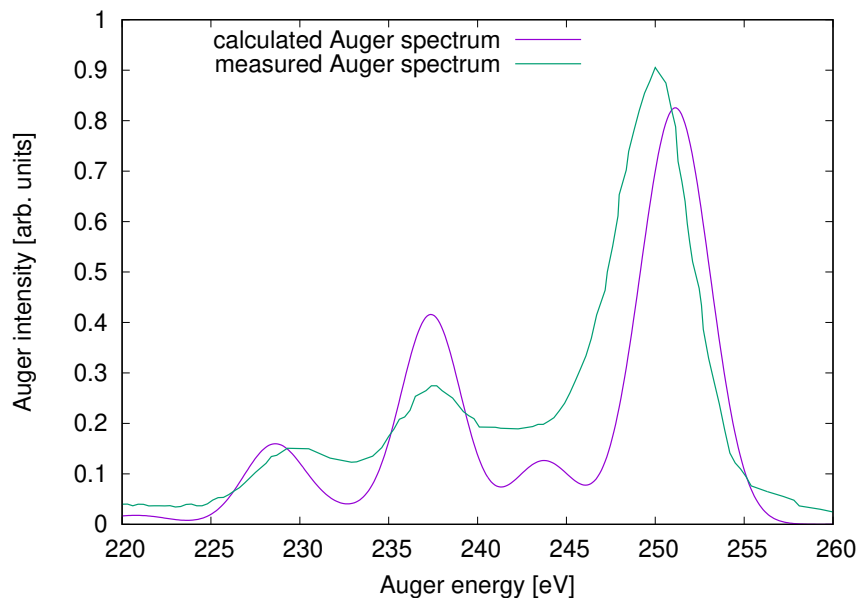

Figure S2: Comparison of calculated and measured AES. Experimental data extracted from Ref. 5.

We further compare calculated AES for methane with available experimental data extracted from Ref. 5. For a better comparison, we convoluted the spectrum with Gaussians of 4eV full width at half maximum and slightly shifted the calculated spectrum by 1.5 eV to lower energies. As can be seen in Fig. S2, the resulting spectrum reproduces all the qualitative features of the experimental Auger spectrum.

XPS signature convolved with experimental time resolution

Based on our simulations in Fig. 2b of the main paper, we simulated the signatures which would be observable in an experiment with finite time resolution. Usually, the time resolution of a optical/free-electron-laser experiments is determined by three components, the duration of the optical laser pulses, the duration of the x-ray pulses, and, either the shot-by-shot jitter of their relative timing or the precision to which this jitter can be measured and corrected for. UV laser pulses with durations
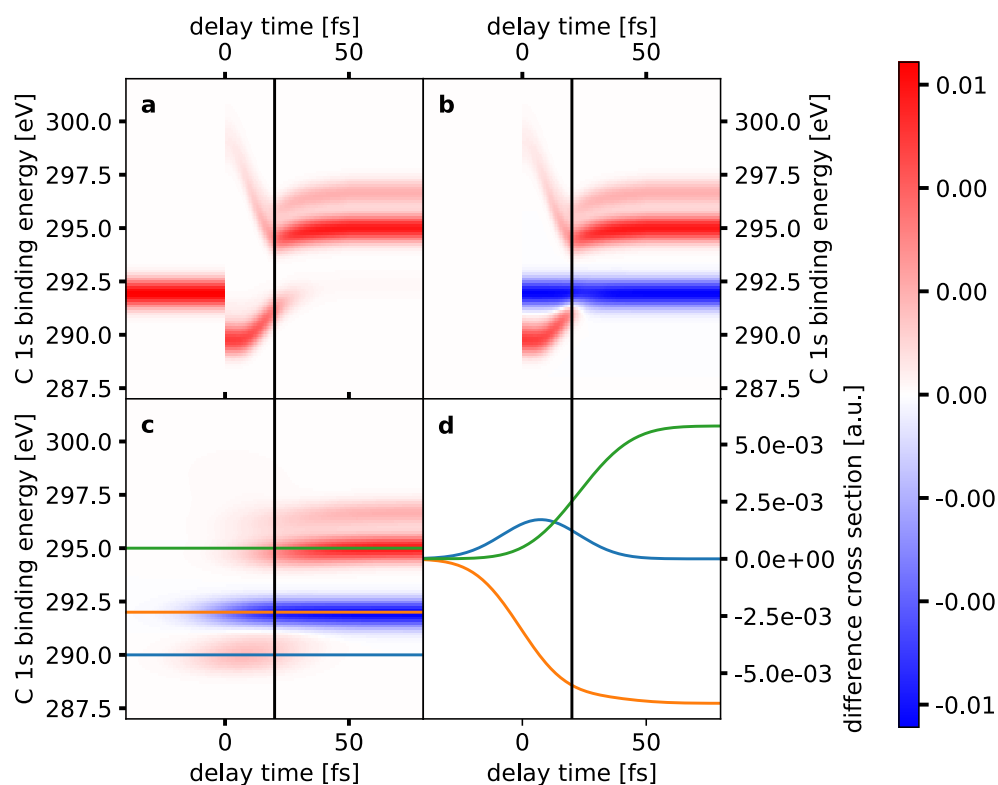
Figure S3: Simulation of time-resolved XPS spectra assuming Gaussian UV and x-ray pulses with a cross-correlation of 35 fs full width at half maximum (FWHM). a) Time-resolved XPS-spectrum assuming delta functions for the time profiles of pump and probe pulse. In comparison to Fig. 2b in the main paper, the ground state XPS spectrum of CH_3I is added for negative time delays.b) Same spectrum as a), but with the ground state XPS spectrum subtracted. The ground state contribution now appears as a negative contribution at positive time delays. c) Same spectrum as b), but convoluted with 35 fs FWHM Gaussian. d) Time-dependence at different positions of the difference spectrum in c), 290 eV (blue), 292 eV (orange), and 295 eV (green).

≤30 fs can be created without substantial effort. Many free electron lasers offer pulse durations down to ≤ 10 fs at appreciable intensities. The timing jitter between optical and x-ray pulses can be measured with 20 fs accuracy. In combination, this results in an achievable time resolution of 35 fs. In Fig. S3a we are showing a time-dependent XPS spectrum assuming 100% excitation and a delta function temporal profile of UV and x-ray pulses. It shows the ground state spectrum of CH_3I for negative time delays and the signatures of the bond dissociation from Fig.2b of the main paper at positive delays. Fig. S3b shows the result of subtracting the ground state XPS spectrum from the spectrum in Fig. S3a. This is a common representation of experimental data in time-resolved x-ray spectroscopy. Here the relative intensities of spectral features are independent of the ratio of photoexcited molecules vs. molecules in the ground state. The ground state XPS spectrum now appears as a negative signature for positive time delays. In Fig. S3c, the difference spectrum from Fig. S3b is convoluted with a Gaussian of 35 fs full width at half maximum in time, which accounts for the achievable experimental time resolution discussed above. At realistic time resolutions, the shift of the strong excited state XPS feature starting at 290 eV to higher binding energies as well as the shift of the weak satellite feature starting at 299.5 eV to lower binding energies are washed out. However, the switch in XPS cross-sections from the main excited state feature at early times to the satellite feature at later times is still well observable. Fig. S3d shows lineouts from Fig. S3c. Time zero is clearly visible in the onset of the negative ground state bleach feature at 292 eV and the initially intense positive feature at 290 eV binding energy. The switch in cross-section 20 fs after UV excitation, marked by a vertical black line, is clearly visible in the decay of the 290 eV feature and the delayed onset of the positive feature at 295 eV.

Classical model of charge transfer

The CH_3 and I in the neutral CH_3I molecule have partial charges $-\delta q$ (CH_3) and δq (I), where $\delta q = 0.15$ is determined from the Mulliken charge analyses at Hartree-Fock level, since the cation after screening-induced charge migration is correlated with the $CH_3 + I^+$ asymptote, we assume that
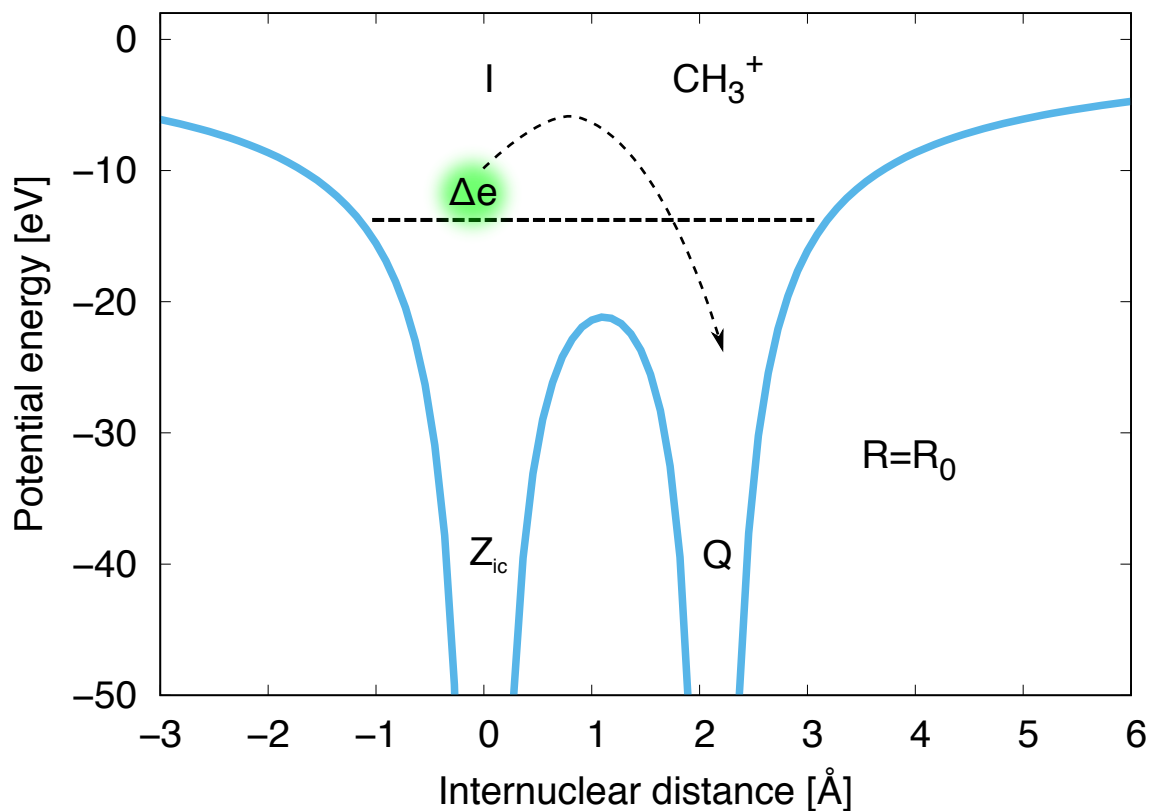
Figure S4: The illustration of potential and the charge (green sphere) to be transferred from iodine to the core ionized CH_3^+. $Z_{ic} = 1$ is the charge of the ion core of I, and $Q = 0.85$ is the partial charge of CH_3^+. The dashed line represents the energy of the lowest bound electron in I atom, which is to be transferred to CH_3^+, which is $E_b = -IP - |\Delta e|Q/R$, and $R = R_0 = 2.136$ Å, $\Delta e = -0.85$.
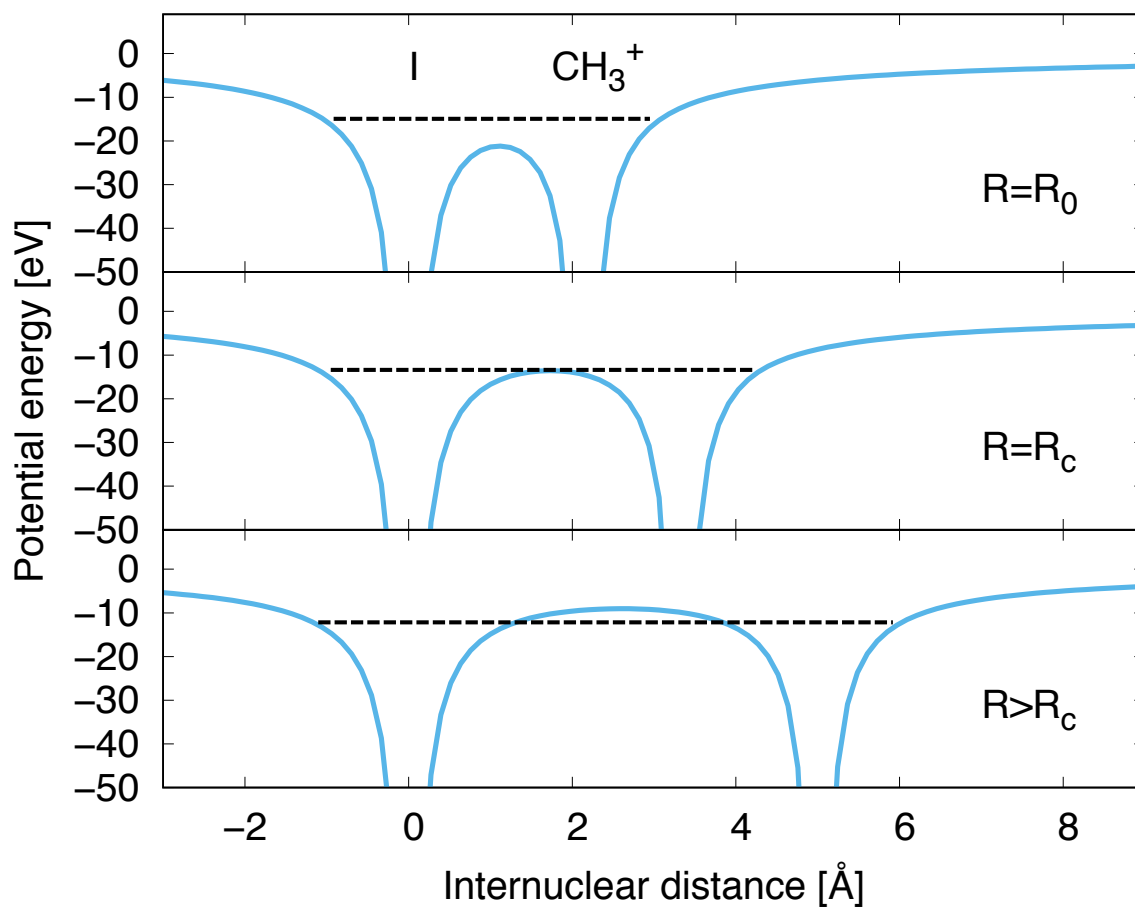
Figure S5: The evolution of internuclear potential experienced by the charge to be transferred from iodine to the core ionized CH_3^+, for internuclear distance R to be the CH_3I equilibrium distance $R_0 = 2.136$ Å, the critical distance $R_c = 3.3$ Å and $R = 5.0$ Å.

fractional charge $\Delta e = -0.85$ is transferred from I to CH_3, leaving behind an ion core I^+ of charge $Z_{ic} = 1$. The partial charge of CH_3^+ before relaxation is $Q = 1 - \delta q = 0.85$, and the fractional charge is transferred in the potential shown in Fig. S4

$$V(x) = -\frac{|\Delta e| Z_{ic}}{|x|} - \frac{|\Delta e Q|}{|R - x|}, \tag{S1}$$

where R is the internuclear distance between C and I located at R and 0, and x is the coordinate of the moving charge modeled as point particle in the 1D system. The potential maximal in the internuclear region $0 < x < R$ is found to be at $x_0 = R/[1 + \sqrt{Q/Z_{ic}}]$, and

$$V_m(x_0) = -|\Delta e| \left[\frac{Z_{ic}}{R} + \frac{2\sqrt{Z_{ic}Q}}{R} + \frac{Q}{R} \right]. \tag{S2}$$

Classically, the energy of the lowest bound electron is

$$E_{lbe} = -IP - \frac{|\Delta e| Q}{R}, \tag{S3}$$

where $IP = 10.45$ eV is the 1st ionization energy of iodine atom, and the second term in Eq. S3 is the perturbative energy from the CH_3^{Q+} ion before charge migration. The charge migration requires naturally the condition $E_{lbe} \geq V_m(x_0)$ (see Fig. S5), it gives the expression of the critical internuclear distance R_c

$$R \leq R_c = |\Delta e| \left[\frac{Z_{ic} + 2\sqrt{Z_{ic}Q}}{IP} \right], \tag{S4}$$

which is calculated to be $R_c = 3.3$ Å.

References

(1) Erk, B. et al. Imaging Charge Transfer in Iodomethane upon X-Ray Photoabsorption. *Science* **2014**, *345*, 288–291.

(2) Ryufuku, H.; Sasaki, K.; Watanabe, T. Oscillatory Behavior of Charge Transfer Cross Sections as a Function of the Charge of Projectiles in Low-Energy Collisions. *Phys. Rev. A* **1980**, *21*, 745–750.

(3) Bakke, A. A.; Chen, H.-W.; Jolly, W. L. A Table of Absolute Core-Electron Binding-Energies for Gaseous Atoms and Molecules. *J. Electron. Spectrosc. Relat. Phenom.* **1980**, *20*, 333–366.

(4) Creber, D. K.; Tse, J. S.; Bancroft, G. M. Experimental and Theoretical Shakeup Studies. III. The 1s Shakeup in CH4, NH3, and H2O. *J. Chem. Phys.* **1980**, *72*, 4291–4299.

(5) Kivimäki, A.; Neeb, M.; Kempgens, B.; Köppe, H. M.; Bradshaw, A. M. The C 1s Auger Decay Spectrum of the Molecule: The Effects of Vibrational Fine Structure, Double Excitations and Shake-up Transitions. *J. Phys. B: At. Mol. Opt. Phys.* **1996**, *29*, 2701–2709.